Geometry and Stability of Titanium Chloride Species Adsorbed on the (100) and (110) Cuts of the $MgCl_2$ Support of the Heterogeneous Ziegler−Natta Catalysts

Guglielmo Monaco,† Massimiliano Toto,† Gaetano Guerra,‡ Paolo Corradini,† and Luigi Cavallo*,†

Dipartimento di Chimica, Università di Napoli, Complesso Monte S. Angelo, Via Cintia, I-80126 Naples, Italy, and Dipartimento di Chimica, Università di Salerno, Via S. Allende, Baronissi, Salerno, Italy

Received June 6, 2000; Revised Manuscript Received September 20, 2000

ABSTRACT: Possible structures of $TiCl_4$ molecules and $TiCl_3$ fragments adsorbed on (110) and (100) faces of $MgCl_2$, simulated by clusters of different size and shape, have been studied in the framework of density functional theory. For both monomeric $TiCl_4$ and $TiCl_3$, coordination on the (110) face is favored relative to coordination on the (100) face. $TiCl_3$ fragments can bind together on the (100) face either forming or not Ti−Ti bonds, resulting in the formation of polynuclear Ti_nCl_{3n} species. The steric environment of the ending Ti atoms of such polynuclear species, with $n > 2$, is extremely similar to that of the C_2 symmetric sites proposed several years ago for $TiCl_3$-based catalytic systems and presents a strict analogy with the well-established models for isospecific polymerization with catalytic systems based on C_2 symmetric metallocenes. This analogy holds also in the case of a $TiCl_3$ fragment adsorbed on the (110) cut when both of its vicinal positions are occupied. When just one of the vicinal positions is occupied, sites of C_1 symmetry can be formed, which have two minimum-energy structures with distinct positions (inward and outward) for the dangling chlorine. These inward and outward geometries can be expected to interconvert easily, the inward arrangement being favored.

1. Introduction

The world market for polypropylene is currently over 20×10^6 tons, and more than 80% of the global polymer[1] is obtained with heterogeneous Ziegler−Natta catalysts.[2−4] Over the years, these catalysts have evolved from simple $TiCl_3$ crystals into the current systems based on $MgCl_2$ as a support for $TiCl_4$. Different routes have been developed for the preparation of the supported catalysts. The mechanical route is based on comilling $MgCl_2$, $TiCl_4$, and a Lewis base (the so-called internal donor) for several hours. Alternatively, chemical routes can be used both to generate active $MgCl_2$ and to incorporate the Ti compound and the Lewis base. Usually, a $MgCl_2$ precursor is treated with the Lewis base and excess $TiCl_4$ above 80 °C. Among internal donors, aromatic esters (ethyl benzoate in particular), alkoxysilanes, and diethers have been shown to be particularly suitable. Finally, the catalyst is activated by addition of alkylating reducing species—$Al(C_2H_5)_3$ being the most used one—possibly mixed with a second electron donor (the so-called external donor). The resulting active system is of extreme chemical complexity, and the intimate nature of the active sites is still a matter of debate.

The characterization of heterogeneous Ziegler−Natta catalysts has been attempted by means of several experimental approaches,[5−26] but definitive answers have not been achieved yet. As for the support structure, the primary particles of activated $MgCl_2$ are composed of a few irregularly stacked Cl−Mg−Cl sandwiches of the kind shown in Figure 1.[6] Observations on $MgCl_2$ microcrystals by optical microscopy[5] and by HRTEM[12] confirmed the proposed[27] copresence of (100) and (110) lateral cuts. For electroneutrality reasons, these two lateral cuts contain coordinatively unsaturated Mg^{2+} ions with coordination number 4 and 5 on the (110) and (100) cuts, respectively, as shown in Figure 1.

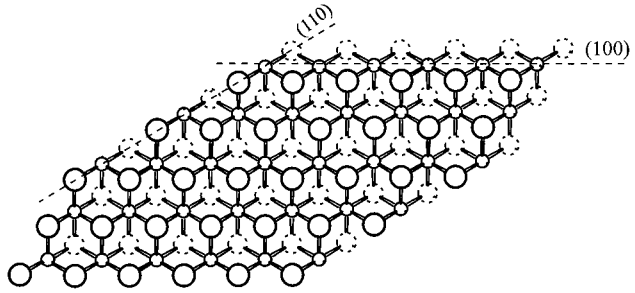

Figure 1. Schematic representation of $MgCl_2$. The full line Cl atoms represent the Cl atoms above the plane of the Mg atoms, whereas the dashed Cl atoms represent the Cl atoms below the plane of the Mg atoms. Possible (100) and (110) lateral cuts with 5- and 4-coordinated Mg atoms are also indicated.

As for treatment with $TiCl_4$, Corradini et al. have proposed that preferential coordination would occur on lateral cuts, leading to adsorbed $TiCl_4$ species on (100) and (110) cuts as well as to adsorbed Ti_2Cl_8 dimers on the (100) cut.[27] In fact, $MgCl_2$ has crystal structures very similar to those of violet titanium trichloride. This dictates the possibility of an epitactical coordination of $TiCl_4$ units (or $TiCl_3$ units, after reduction) on the lateral coordinatively unsatured faces of $MgCl_2$ crystals, giving rise to reliefs crystallographically coherent with the matrix. Moreover, EXAFS studies[7,8] are consistent with this model pointing to the coordination of $TiCl_4$ as a monomer[7] or a dimer on the (100) face.[8]

The knowledge of catalyst structure after reduction with alkylaluminum compounds is also incomplete. As

† Università di Napoli.
‡ Università di Salerno.
* Corresponding author. E-mail: cavallo@chemistry.unina.it.

10.1021/ma000988h CCC: $19.00
Published on Web 11/28/2000

for the Ti oxidation state, literature reports are often contradictory, owing to the different catalysts and analytical methods used.[7,9,13−20] The only reasonable conclusion is that under polymerization conditions a considerable reduction of Ti(IV) takes place, not only to Ti(III) but to Ti(II) as well. However, Ti(II) is usually considered not to be active for propene polymerization.[19] The structure of $TiCl_3$ fragments adsorbed on the support is not known. Similarly to isolated $TiCl_4$ molecules, isolated $TiCl_3$ fragments could be epitactically adsorbed on the (110) and (100) cuts, while dimeric Ti_2Cl_6 species could be grown on the (100) cut. These species could be obtained by direct reduction of the corresponding $TiCl_4$ and Ti_2Cl_8 adsorbed species.[27,28] However, rearrangements of $TiCl_3$ species on the surface are also possible, and ESR experiments suggest the formation of polynuclear species of the type Ti_mCl_n.[17,18] It is also worth noting that these experiments indicate that most of the Ti(III) is ESR silent.[17,18,20]

Useful information on the nature of active sites can also be obtained by ^{13}C NMR analyses of the polymers produced.[28,29] These analyses indicate that some active sites can interconvert in a time shorter than the average time of chain growth[21−26] and that at least one of the active sites has an environment of C_1 symmetry.[24,26]

Although the whole framework is extremely complicated, some theoretical efforts have been attempted in this field. Most of the work concentrated on the elementary steps of the polymerization reaction,[30−34] and the ab initio investigations of Pakkanen and co-workers on the interactions occurring between $TiCl_4$ and/or Lewis bases and $MgCl_2$ clusters represent an exception.[35−39] However, for $TiCl_4$ they investigated small complexes, and thus, although valuable, their study cannot be conclusive. A more detailed study of the interactions between $TiCl_4$ and the (110) $MgCl_2$ face is reported in a paper by Parrinello and co-workers,[40] which used first principles molecular dynamics to investigate possible structures of $TiCl_4$ species adsorbed on the (110) face.[40] They found that $TiCl_4$ can adopt various geometries, the one corresponding to the $TiCl_4$ epitactically grown on the $MgCl_2$ (110) face being the most stable. However, according to the authors, a higher energy 5-coordinated geometry (similar to that already considered by Pakkanen and co-workers)[35] would be kinetically favored.

Considering the remarkable contribution given by first principles computational approaches to the understanding of the behavior of the homogeneous Ziegler−Natta catalysts, we have been spurred to use these tools to study the industrially relevant heterogeneous catalysts. For this reason, in this paper we attempted a systematic density functional theory (DFT) investigation of possible structures formed by adsorption of $TiCl_4$ on both faces of $MgCl_2$, and we also investigated the possible formation of dimeric Ti_2Cl_8 species on the (100) face. We also attempted a characterization of adsorbed Ti species after reduction of Ti(IV) to Ti(III). For this reason, we investigated possible structures of $TiCl_3$ fragments adsorbed on the (110) face and of monomeric, dimeric, and tetrameric $TiCl_3$ species on the (100) face.[41] Since very little is known about these systems at molecular level, only a systematic comparison between the various species involved can be of some use. The main aim of this study is a simple structural and energetical characterization of possible adsorbed Ti species from a static point of view and a consideration of their possible stereospecific behavior. When analyzing the results, it should be remembered that the evaluated energy differences only represent a contribution to the total free energy differences, since solvent and entropic effects are not considered. Moreover, the role of the alkylaluminum and that of the Lewis bases have not been considered. Of course, the presence of these species is needed to achieve an active and highly stereospecific catalyst.[42] However, activation and deactivation (mainly due to reactions of adsorbed Ti species with alkylaluminum compounds and Lewis bases)[42] are out of the scope of the present work, which only focuses on the structure of possible precursors of active sites. For the same reason, adsorption of Ti(II) species has not been considered, since Ti(II) is generally thought to be inactive in propene polymerization.[19] As for the role played by Lewis bases in modifying the catalysts behavior, it has been the subject of a complementary study which has been reported elsewhere.[43]

2. Models and Methods

Except when specifically indicated, the geometry of the $MgCl_2$ clusters has been kept fixed. The Mg−Cl distances and all the Cl−Mg−Cl angles have been set equal to 2.49 Å and 90°.[44] This corresponds to the simplifying assumption that the atoms on the surface present a structure close to that present in the bulk of the crystal. A different approach could consider a total relaxing of all the degrees of freedom. However, due to the dimension of the considered clusters, we think that this last approach would imply deformations that would not be representative of the rearrangements that occur on the $MgCl_2$ surface. To check for the reasonability of these assumptions, test calculations with a partial relaxation of the $MgCl_2$ cluster will also be discussed. With regards to the size of the chosen clusters, we decided to consider only situations in which the Mg atoms that are involved in the coordination of the Ti species should have (previous to Ti adsorption) coordination numbers 4 and 5 on the (110) and (100) lateral cuts, respectively, as requested by electroneutrality reasons (see Figure 1). Moreover, all the Cl atoms of the cluster involved in the coordination of the Ti species should bridge two Mg atoms (see Figure 1). These minimum requirements lead to the Mg_9Cl_{18} and Mg_8Cl_{16} clusters as models for the (100) and (110) lateral cuts, respectively, shown in Figure 2. These clusters represent a reasonable compromise between reliability and computational efficacy. For the sake of consistency, these clusters were used throughout the paper. As we considered adsorption of tetrameric Ti species, however, Mg atoms that do not respect the above requirements are involved. Only for this case, we used the larger $Mg_{13}Cl_{26}$ cluster.

Computational Details. The density functional calculations were carried out by using the Amsterdam Density Functional package ADF, developed by Baerends et al.[45−47] The geometry optimization procedure has been developed by Versluis and Ziegler.[48] The electronic configurations of the systems were described by an uncontracted triple-ζ STO basis set on Ti(3*s*, 3*p*, 3*d*, 4*s*, 4*p*) and Mg(3*s*, 3*p*, 3*d*).[49] A double-ζ STO basis sets augmented with a single 3d polarization function was used for Cl(3*s*, 3*p* + 3*d*).[49] The $1s^22s^22p^6$ configuration on Ti, Mg, and Cl was treated by the frozen-core approximation. Energies and geometries have been obtained by using the local potential by Vosko et al.,[50] augmented in a self-consistent manner by the Becke's exchange gradient correction[51] and by the Perdew's correlation gradient correction.[52,53] Whenever systems with unpaired electrons were considered, an unrestricted formalism has been used.

Although transition metal−ligand dissociation energetics obtained with the DFT approach outlined above have been shown to be correct within 5 kcal/mol of the experimental result (usually overestimated in terms of absolute size),[54,55] for bridged-bonded aluminum compounds DFT methods have been shown to underestimate the heats of formation.[56] However, a recent comparative computational study has shown

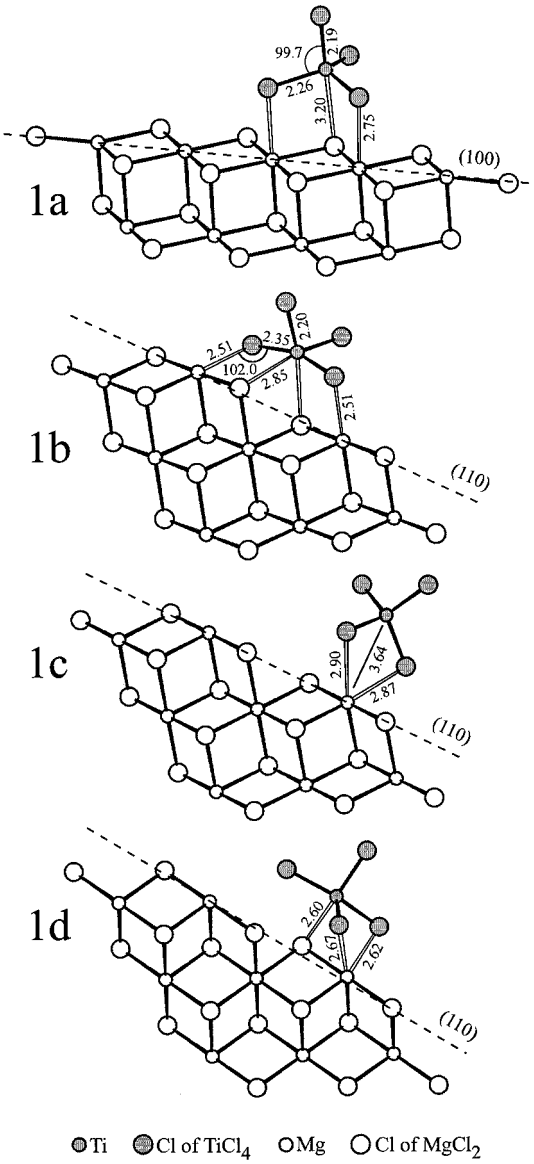

Figure 2. Optimized geometries of structures **1a**, **1b**, **1c**, and **1d**, corresponding to a $TiCl_4$ molecule adsorbed on the (100) face of a Mg_9Cl_{18} cluster, and to 6-fold, 4-fold and 5-fold $TiCl_4$ molecules adsorbed on the (110) face of a Mg_8Cl_{16} cluster, respectively. Only the positions of the $TiCl_4$ atoms have been optimized. **1d** has been obtained without inclusion of exchange-correlation gradient corrections (see methods). Hollow bonds are used to indicate bonds between the $TiCl_4$ and the Mg_8Cl_{16} cluster.

that the DFT functional we have chosen is in excellent agreement with the high-level CSSD(T) coupled cluster calculations performed by Jensen and Bøtve.[57]

Energy Decomposition. In this paper we will be concerned with the adsorption of groups of $TiCl_4$ molecules and/or $TiCl_3$ fragments on supports, S, formed by $MgCl_2$ clusters. We will indicate as binding energy per Ti atom, E_B, of a given group of species {A} only the electronic contribution to the binding free energy G_B. The free and adsorbed species can be expected to have markedly different nonelectronic contribution to their free energy. Therefore, the values computed for E_B cannot be used to determine the percentage of adsorbed species. However the relative binding energies can be expected to be substantially more reliable[58] and can be reasonably used to get an idea of the preferred arrangements of the adsorbed species.

For a given group of species {A} and a given support S, the binding energy E_B per Ti atom is computed as

$$E_B = (E_{\{A\}} + E_S - E_{\{A\}/S})/m \quad (1)$$

where $E_{\{A\}}$, E_S, and $E_{\{A\}/S}$ are the electronic energies of the isolated species which compose {A}, of the isolated support (either relaxed or unrelaxed) and of the system formed upon adsorption of the Ti species, respectively, while m is the number of Ti atoms present in {A}.

Relative binding energies ΔE_B have been computed assuming two reference structures: $TiCl_4$ and $TiCl_3$ adsorbed on a cluster that simulates the (100) face. The sign convention is such that positive ΔE_B correspond to energy gain.

Often the adsorption leads to a significant change of the geometry. To investigate the influence that such change in geometry has on the values of the adsorption energies, the binding energy has been decomposed as follows:[59]

$$E_B = E_{Intra} + E_{Inter} \quad (2)$$

where $E_{Inter} = (E^*_{\{A\}} + E^*_S - E_{\{A\}/S})/m$ is the energy per Ti atom needed to dissociate the adsorbed species {A} avoiding any relaxation from the geometry found upon adsorption, and $E_{Intra} = E_{Intra\{A\}} + E_{Intra(S)}$ is the sum of the energy contributions $(E_{\{A\}} - E^*_{\{A\}})/m$ and $(E_S - E^*_S)/m$ required to restore the equilibrium geometry of the adsorbed species and that of the support. Excluding two test calculations, the geometry of the support has been kept fixed and thus $E_S = E^*_S$.

3. Results and Discussion

The starting points of our calculations have been the models of epitactic adsorption of Ti chlorides species proposed long ago by Corradini et al.[27] As will be seen, the geometries found in the calculations are generally very similar to epitactic models, although there are deviations that are of interest. These deviations can be attributed to the fact that the length of a Ti−Cl bond (∼2.2 Å) is considerably shorter than the length of a Mg−Cl bond (∼2.5 Å), and thus epitactic placements require a deformation of the adsorbates (negative E_{Intra}). Moreover, unbridged Cl atoms have a stronger trans influence than bridged ones,[60] and this is a further source of deformation. To get an easy visualization of the deformations, it is possible to focus only on the shortest Ti−Cl bonds (say shorter than ∼3 Å). Finally, the relative binding energies (ΔE_B) calculated for Ti(IV) (upper part) and Ti(III) (lower part) species on (100) and (110) lateral cuts are collected in Table 1, together with their intramolecular (ΔE_{Intra}) and intermolecular (ΔE_{Inter}) contributions.

Adsorption of Ti(IV) Species. The optimized geometry of a $TiCl_4$ molecule epitactically adsorbed on the (100) face of the $MgCl_2$ cluster **1a** is reported in Figure 2. The geometry around the Ti atom is a strongly distorted trigonal bipyramid, with the axis almost perpendicular to the (100) face. The long bond distances Ti−Cl(surface) and Mg−Cl($TiCl_4$) suggest a weak interaction between the $TiCl_4$ molecule and the $MgCl_2$ cluster. Since there are only four "short" Ti−Cl bonds, an alternative description of the geometry is that of a distorted tetrahedron. In the following, **1a** will be the reference state at 0 kcal/mol for the adsorption of $TiCl_4$ molecules.

In agreement with previous hypotheses[27] and with the findings of Parrinello,[40] the most stable geometry of a $TiCl_4$ molecule epitactically adsorbed on the (110) face of the $MgCl_2$ cluster **1b** presents the Ti atom octahedrally coordinated. The $TiCl_4$ molecule is considerably closer to the $MgCl_2$ surface relative to **1a**, and the better $TiCl_4$/support interaction is confirmed by the high ΔE_B (8.3 kcal/mol). We also tried to optimize a $TiCl_4$ molecule

Table 1. Energy Decomposition of Total Binding Energies, ΔE_B

label	adsorbed species	unpaired spins	cluster[a,j]	ΔE_{intra},[b] kcal/mol	ΔE_{inter},[c] kcal/mol	ΔE_B[d] (E_B[e]), kcal/mol
1a	$TiCl_4$	0	(100)−1a	0	0	0 (5.0)
1b	6-fold $TiCl_4$	0	(110)−1b	−20.5	28.8	8.3 (13.3)
	6-fold $TiCl_4$	0	(110)−2b	−20.4	30.7	10.3 (15.3)
1c	4-fold $TiCl_4$	0	(110)−1b	4.9	−4.5	0.4 (5.4)
2a	Ti_2Cl_8	0	(100)−1a	−8.4	9.8	1.4 (6.4)
2b	two $TiCl_4$	0	(110)−2b	−21.2	25.6	9.4 (14.4)
3a	$TiCl_3$	1	(100)−1a	0	0	0 (24.9)
3b	$TiCl_3$	1	(110)−1b	−8.7	13.6	4.9 (29.8)
4in	$TiCl_4$−$TiCl_3$	1	(110)−4in	−19.6,[f] −9.7[g]	24.5	5.7 (24.8)
4out	$TiCl_4$−$TiCl_3$	1	(110)−4in	−19.4,[f] −13.1[g]	23.9	3.5 (22.6)
5	Ti_2Cl_7	1	(100)−1a	−1.7	−7.6	1.0 (15.9)
7-*S*0	Ti_2Cl_6	0	(100)−1a	3.2	−4.6	−1.4 (23.5)
7-*S*2	Ti_2Cl_6	2	(100)−1a	6.7	−7.7	−1.0 (23.9)
9-*S*0	Ti_2Cl_6	0	(100)−1a	2.3,[h] −18.6[i]	0.7	−6.1 (18.2)
9-*S*2	Ti_2Cl_6	2	(100)−1a	3.3,[h] −21.3[i]	1.3	−5.5 (18.8)
8-*S*0	Ti_4Cl_{12}	0	(100)−1a	12.6	−11.5	1.1 (26.0)
8-*S*4	Ti_4Cl_{12}	4	(100)−1a	12.2	−10.8	1.4 (26.3)
	Ti_4Cl_{12}	0	(100)[j]	11.5	−8.9	2.6 (27.5)
	Ti_4Cl_{12}	4	(100)[j]	11.9	−8.9	3.0 (27.9)

[a] The different clusters used to simulate the lateral cuts are labeled with the Miller indices of the considered cut and with the name of first species in which the clusters are present. [b] ΔE_{Intra} is the energy difference between E_{Intra} per Ti atom of the Ti_mCl_n species and E_{Intra} of monomeric $TiCl_4$ and/or $TiCl_3$ adsorbed on the (100) cut, which amount to −5.8 and −6.7 kcal/mol, respectively. [c] ΔE_{Inter} is the energy difference between E_{Inter} per Ti atom of the Ti_mCl_n species and E_{Inter} of monomeric $TiCl_4$ and/or $TiCl_3$ adsorbed on the (100) cut, which amount to 10.8 and 31.6 kcal/mol, respectively. [d] ΔE_B is the energy difference between E_B per Ti atom of the Ti_mCl_n species and E_B of monomeric $TiCl_4$ and/or $TiCl_3$ adsorbed on the (100) cut. [e] Absolute binding energies per Ti atom with respect to isolated $MgCl_2$ clusters and $TiCl_4$ molecules and/or $TiCl_3$ fragments. [f] ΔE_{Intra} of the $TiCl_4$ molecule. [g] ΔE_{Intra} of the $TiCl_3$ fragment. [h] ΔE_{Intra} per Ti atom of the Ti_2Cl_6 species. [i] Unnormalized ΔE_{Intra} of the $MgCl_2$ cluster. [j] A $Mg_{13}C_{26}$ cluster, obtained by symmetrical lengthening of the (100)-1a cluster, has been used.

adsorbed on the (110) face with a 5-fold-coordinated Ti atom, similar to those proposed by Pakkanen[35] and Parrinello.[40] All the performed attempts led to **1c**, which essentially corresponds to an undeformed $TiCl_4$ molecule slightly interacting with the $MgCl_2$ cluster (ΔE_B 0.4 kcal/mol). Since the molecular dynamics simulations of Parrinello were performed without the inclusion of gradient corrections and were checked with gradient corrected static calculations by using the Becke−Lee−Yang−Parr level of theory,[61] we performed a further geometry optimization without including the Becke−Perdew gradient corrections.[51−53] In this case, the geometry optimization converged to the 5-fold geometry **1d**, very similar to that proposed by Parrinello.[62]

The $TiCl_4$ dimer, Ti_2Cl_8, coordinated to the (100) face of the $MgCl_2$ cluster, **2a**, represents a stable structure of C_s symmetry with two Cl atoms forming bridges between the two octahedrally coordinated Ti atoms, in agreement with models proposed several years ago.[27] The Ti_2Cl_8 fragment is closer to the $MgCl_2$ surface relative to the $TiCl_4$ monomer, and the calculated Ti−Ti and Ti−Cl(surface) distances (3.89 and 2.75 Å, respectively) are in reasonable agreement with the corresponding distances of a model derived from an EXAFS spectrum analysis (3.7 and 3.0 Å, respectively).[8] ΔE_B amounts to 0.7 kcal/mol, indicating a good interaction between the Ti_2Cl_8 fragment and the $MgCl_2$ cluster and that the formation of dimeric Ti_2Cl_8 species is favored relative to the adsorption of isolated $TiCl_4$ molecules. Two such molecules adsorbed on vicinal coordination sites on the (110) face, **2b**, also represent a stable situation. In fact, ΔE_B per $TiCl_4$ molecule is only 0.9 kcal/mol smaller than ΔE_B of an isolated $TiCl_4$ molecule on the same $MgCl_2$ cluster.

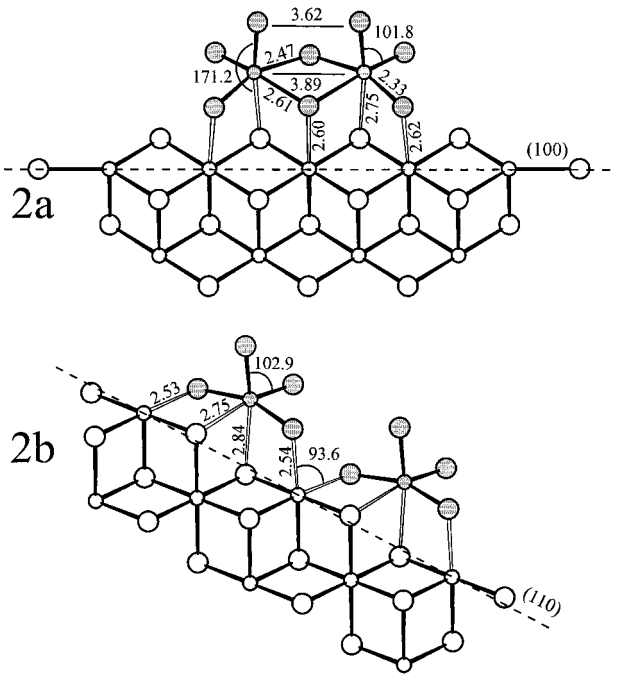

Figure 3. Optimized geometries of structures **2a** and **2b**, corresponding to a Ti_2Cl_8 fragment adsorbed on the (100) face of a Mg_9Cl_{18} cluster and to two $TiCl_4$ molecules adsorbed on vicinal coordination positions on the (110) face of a Mg_8Cl_{16} cluster, respectively. Only the positions of the Ti_2Cl_8 atoms and of the two $TiCl_4$ molecules have been optimized. Hollow bonds are used to indicate bonds between the Ti_2Cl_8 fragment or the two $TiCl_4$ molecules and the Mg_9Cl_{18} cluster.

Adsorption of Ti(III) Species. The lowest energy geometry of the system obtainable after reduction of adsorbed $TiCl_4$ and consisting of a $TiCl_3$ fragment adsorbed on the (100) face of the $MgCl_2$ cluster, **3a**, shows the Ti atom tetrahedrically coordinated and short Ti−Cl(surface) and Mg−Cl($TiCl_3$) distances.[41] In the following, **3a** will be the reference state at 0 kcal/mol for structures with adsorbed $TiCl_3$ fragments. The structure composed by a $TiCl_3$ fragment adsorbed on the (110) face of the $MgCl_2$ cluster, **3b**, has a ΔE_B value, 4.9 kcal/mol, which suggests a better interaction between the $TiCl_3$ fragment and the (110) $MgCl_2$ cut.

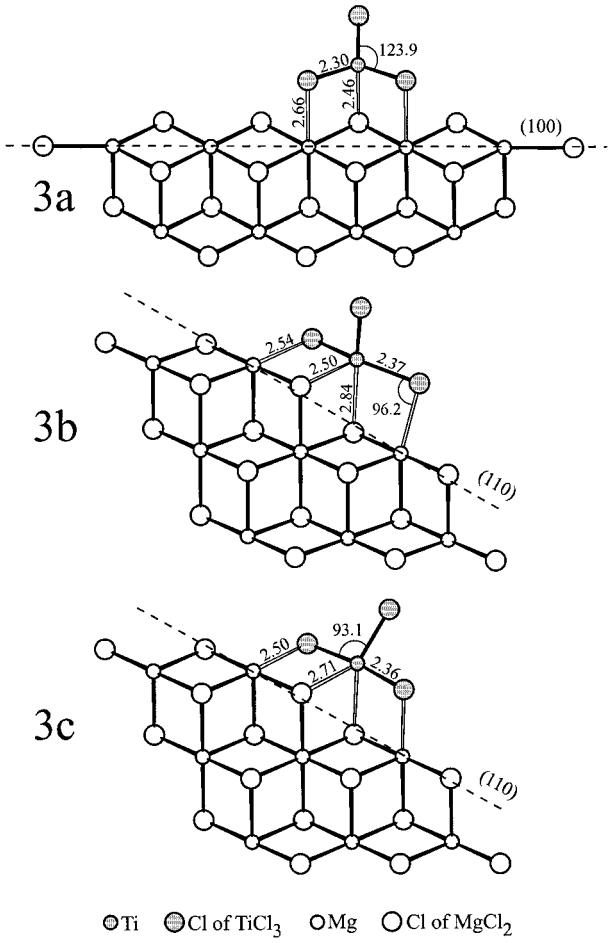

Figure 4. Optimized geometries of structure **3a** corresponding to a $TiCl_3$ fragment adsorbed on the (100) face of a Mg_9Cl_{18} cluster and of structures **3b** and **3c** corresponding to C_1 and a C_2 symmetric $TiCl_3$ fragments adsorbed on the (110) face of a Mg_8Cl_{16} cluster, respectively. Structure **3c** corresponds to a transition state. Only the positions of the $TiCl_3$ atoms have been optimized. Hollow bonds are used to indicate bonds between the $TiCl_3$ fragment and the Mg_9Cl_{18} cluster.

Structure **3b** is highly asymmetric, and the geometry around the Ti atom is a distorted octahedron with a vacant coordination position. The removal of a chlorine atom from the parent structure **1b** results in the loss of a trans influence and thus in the remarkable shortening of a Ti−Cl(surface) distance. Moreover, it can be noted that one of the Cl atoms forming a Ti−Cl−Mg bridge has a position that differs significantly from the epitactical one. This leads to different geometries for the two vicinal magnesium atoms: a square pyramid and a trigonal bipyramid. The asymmetry of **3b** implies the existence of another minimum (equivalent by symmetry), in which the only dangling chlorine occupies the vacant coordination position on the Ti atom of **3b**. The transition state, **3c**, for the switch between these two situations has a C_2 symmetry and has a higher energy relative to the minima of only 3.3 kcal/mol, thus suggesting a fast interconversion. When a $TiCl_4$ molecule is coordinated adjacent to **1b**, we obtain two minima that are no longer equivalent. In fact, the $TiCl_4$ molecule can be adsorbed on the side of the square-pyramidal magnesium atom or on the side of the trigonal-bipyramidal magnesium atom. In analogy with previous works,[28] the two structures will be named inward and outward, **4in** and **4out**, respectively. Despite the presence of a repulsive interaction between the

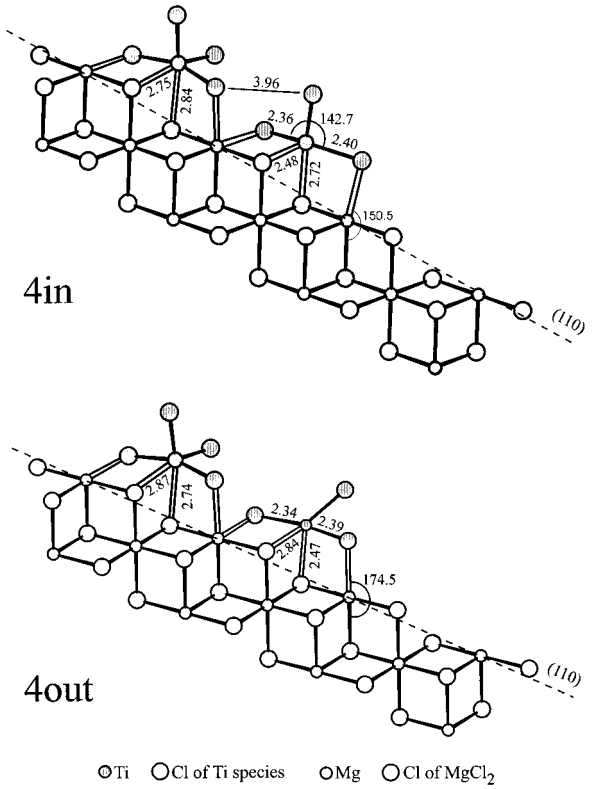

Figure 5. Optimized geometries of structures **4in** and **4out**, corresponding to the adsorption of a $TiCl_3$ fragment and a $TiCl_4$ molecule on the (110) face of a $Mg_{11}Cl_{22}$ cluster. The main difference between the two structures is the orientation of the dangling chlorine of the $TiCl_3$ fragment. Only the positions of the Ti chloride species have been optimized.

$TiCl_4$ molecule and the dangling Cl atom of the $TiCl_3$ fragment, **4in** is favored by 4.4 kcal/mol relative to **4out**. This preference can be ascribed to the deformation of the $TiCl_3$ fragment, since the deformation energy of the $TiCl_3$ fragment in **4in** is 3.4 kcal/mol higher than in **4out**, which compares well with the difference in the binding energy reported above. Beside the monomer $TiCl_3$, it is possible to imagine different structures arising from the reduction of adsorbed Ti(IV) species. Starting form the dimer Ti_2Cl_8, progressive reduction to Ti(III) would lead to Ti_2Cl_7 and finally to Ti_2Cl_6.

The ΔE_B corresponding to the optimized geometry of a Ti_2Cl_7 species adsorbed on the (100) face, **5**, indicates a preference over an isolated $TiCl_4$ molecule and an isolated $TiCl_3$ fragment adsorbed on the same face. The geometry of the pentacoordinated Ti(III) is similar to a trigonal bipyramid; i.e., the dangling chlorine lies in the middle of the two octahedral positions, as expected.[30,32−34,63] Upon further reduction, a Ti_2Cl_6 species can be formed. Although in this paper we are concerned with geometry and stability of adsorbed species, a few remarks on isolated Ti_2Cl_6 species are useful. Therefore, we considered the structures of free Ti_2Cl_6 species with zero and two unpaired electron spins, **6-*S*0** and **6-*S*2**, respectively. The formation energy of **6-*S*0** and **6-*S*2** relative to free $TiCl_3$ fragments is −37.0 and −29.3 kcal/mol, respectively, with **6-*S*0** favored by 7.7 kcal/mol with respect to **6-*S*2**. The main feature of **6-*S*0** is the presence of a Ti−Ti bond. In structure **6-*S*2**, instead, the Ti−Ti distance is longer due to the absence of a Ti−Ti bond and to repulsive interactions between the two singly occupied orbitals which are oriented along the Ti−Ti axis.[64] The structures composed by Ti_2Cl_6 coordinated

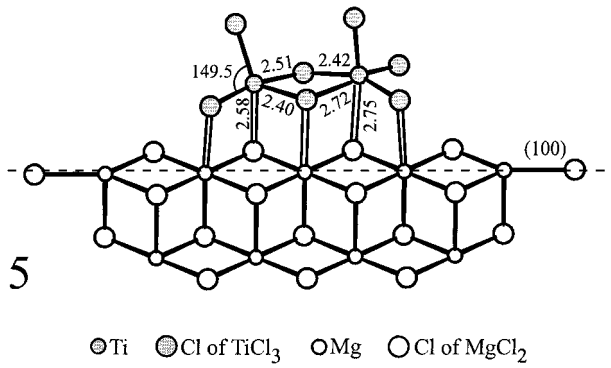

Figure 6. Optimized geometry of structure **5**, corresponding to the Ti_2Cl_7 fragment adsorbed on the (100) face of a Mg_9Cl_{18} cluster. Only the positions of the Ti_2Cl_7 atoms have been optimized. Hollow bonds are used to indicate bonds between the Ti_2Cl_6 fragment and the Mg_9Cl_{18} cluster.

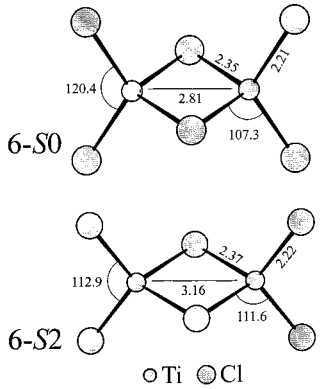

Figure 7. Optimized geometries of structures **6-*S*0** and **6-*S*2**, corresponding to the free Ti_2Cl_6 fragment.

to the (100) face of the $MgCl_2$ cluster, with zero and two unpaired electron spins, **7-*S*0** and **7-*S*2**, respectively, represent stable structures of C_s symmetry. In structure **7-*S*0** the Ti−Ti bond distance is stretched by only 0.12 Å with respect to the same distance in the free **6-*S*0** Ti_2Cl_6 model species. In structure **7-*S*2**, instead, the Ti−Ti distance is 0.55 Å longer with respect to the same distance in the free **6-*S*2** Ti_2Cl_6 species. In both structures the geometry of the Ti is a distorted trigonal bipyramid, as expected.[30,32−34,63] It is interesting to note that the deviations of the dangling Cl atoms from the middle positions are opposite in the two structures, being more perpendicular or parallel to the surface. The ΔE_B per Ti atom of **7-*S*0** and **7-*S*2** amount to −1.4 and −1.0 kcal/mol, respectively, with **7-*S*2** slightly favored. The preference for the ***S*2** geometry upon coordination is probably due to the absence of a Ti−Ti bond, which allows for a greater flexibility of the Ti_2Cl_6 fragment, which can easily adopt a geometry apt to be bonded on the surface. For Ti(IV), the dimeric species **2a** is the larger cluster that can be grown on the $MgCl_2$ (100) face, whereas after Ti(IV) reduction to Ti(III) also larger clusters could be formed in principle. The optimized geometries of Ti_4Cl_{12} adsorbed on the (100) face of the $MgCl_2$ cluster, with zero and four unpaired electron spins, are denoted **8-*S*0** and **8-*S*4**, respectively.[67] Structure **8-*S*0** presents an alternance of short−long−short Ti−Ti distances, which are very close to the Ti−Ti distances calculated for the coordinated Ti_2Cl_6 fragments **7-*S*0** and **7-*S*2**, respectively. This suggests that **8-*S*0** can be considered as composed by two Ti_2Cl_6 fragments presenting a Ti−Ti bond and no unpaired electron spins, connected by two bridging Cl atoms.

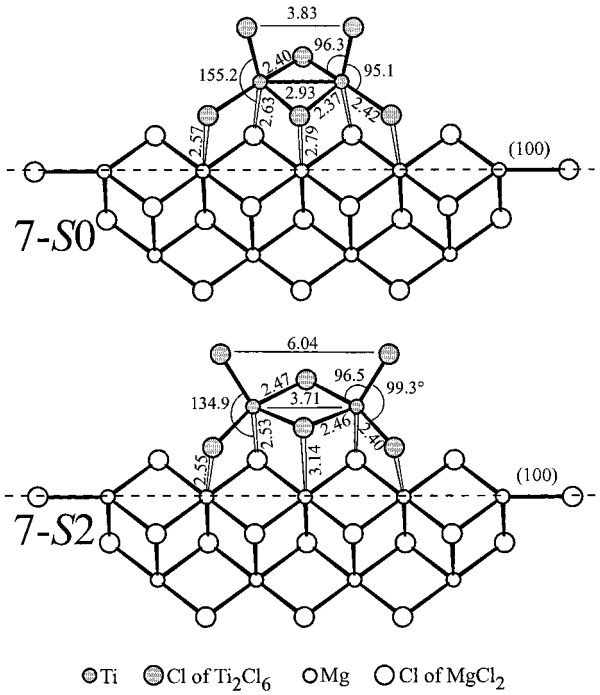

Figure 8. Optimized geometries of structures **7-*S*0** and **7-*S*2**, corresponding to the Ti_2Cl_6 fragment adsorbed on the (100) face of a Mg_9Cl_{18} cluster. Only the positions of the Ti_2Cl_6 atoms have been optimized. Hollow bonds are used to indicate bonds between the Ti_2Cl_6 fragment and the Mg_9Cl_{18} cluster.

Structure **8-*S*4**, instead, presents Ti−Ti distances much more similar to each other, with the central Ti−Ti distance only longer by 0.17 Å. This suggests that **8-*S*4** can be considered as composed by four $TiCl_3$ fragments connected by bridging Cl atoms. The ΔE_B per Ti atom amounts to 1.1 and 1.4 kcal/mol for **8-*S*0** and **8-*S*4**, respectively. As for the case of the dimeric structures **7-*S*0** and **7-*S*2**, situations with different number of unpaired spins are of similar energy. Since Ti_4Cl_{12} adsorption in structures **7-*S*0** and **7-*S*2** involves Mg atoms that (previous Ti_4Cl_{12} coordination) are not characterized by a coordination number 5, we decided to make test calculations by considering Ti_4Cl_{12} coordination on the bigger $Mg_{13}Cl_{26}$ cluster and reported in the last two coloumns of Table 1. These calculations indicated that while E_B are somewhat dependent from the cluster size, ΔE_B are quite more stable. In fact, the adsorbed Ti_4Cl_{12} species with 0 unpaired spins is slightly more stable than the same species with 4 unpaired spins, also with the $Mg_{13}Cl_{26}$ cluster. The relative binding energies (ΔE_B) calculated for Ti(IV) (upper part) and Ti(III) (lower part**)** species on (100) and (110) lateral cuts are collected in Table 1, together with their intramolecular (ΔE_{Intra}) and intermolecular (ΔE_{Inter}) contributions, which generally are considerably larger than the corresponding ΔE_B.

To check for the effects due to the relaxation of the atoms at the surface of the (100) $MgCl_2$ cut, we partially optimized the geometry of the Mg_9Cl_{18} cluster without, **9**, and with coordinated Ti_2Cl_6 fragments with zero and two unpaired electron spins, **9-*S*0** and **9-*S*2**, respectively. The optimized atoms are those enclosed in the dashed boxes. In agreement with the results of Parrinello and co-workers,[40] we noticed a tendency of the Cl atoms to stretch out of the $MgCl_2$ surface, resulting in a partial screening of the unsaturated Mg atoms. Structures **9-*S*0** and **9-*S*2** are quite similar to **7-*S*0** and

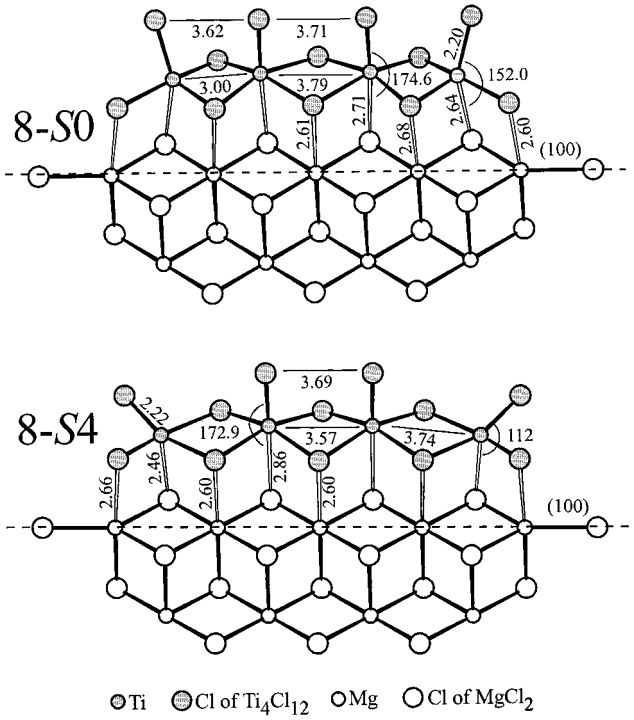

Figure 9. Optimized geometries of structures **8-*S*0** and **8-*S*4**, corresponding to the Ti_4Cl_{12} fragment adsorbed on the (100) face of a Mg_9Cl_{18} cluster. Only the positions of the Ti_4Cl_{12} atoms have been optimized. Hollow bonds are used to indicate bonds between the Ti_4Cl_{12} fragment and the Mg_9Cl_{18} cluster.

7-*S*2, respectively, supporting the reliability of our models. The binding of the Ti_2Cl_6 fragment to the $MgCl_2$ cluster in **9-*S*0** and **9-*S*2** is weaker by roughly 10 kcal/mol relative to those in **7-*S*0** and **7-*S*2**. However, also for these more relaxed models the ***S*2** structure is slightly favored, by 0.6 kcal/mol, relative to the ***S*0** structure. This implies that although the absolute E_B obtained with fixed $MgCl_2$ clusters are overestimated, the energy differences between different structures seem to be substantially independent from a relaxation of the $MgCl_2$ clusters.

Discussion. Although we have calculated only electronic contributions to the binding free energies, it can be reasonably expected that the relative binding energy data reported in Table 1 can be used to gain insights into the species which can be more probably formed during catalyst preparation.

First of all, coordination on the (110) face is favored relative to coordination on the (100) face for both $TiCl_4$ molecules and $TiCl_3$ fragments. This is in good qualitative agreement with the higher acidity of the magnesium atoms of the (110) face, as estimated from simple electrostatic calculations.[27] In effect, the preferential binding to the (110) face is essentially related to the high attractive intermolecular contributions which more than counterbalance the destabilizing intramolecular contributions (cf. E_{Inter} and E_{Intra} values of **1a** and **3a** with those of **1b** and **3b**, respectively).

As for the (110) lateral cut, Ti(IV) and Ti(III) would be bound preferentially as isolated $TiCl_4$ molecules and $TiCl_3$ fragments, i.e., **1b** and **3b**, respectively. However, a small energy is required to obtain adjacent monomeric species (like **2b** or **4**).

As for the (100) lateral cut, besides the isolated $TiCl_4$ and $TiCl_3$ species **1a** and **3b**, dimeric Ti_2Cl_8 and Ti_2Cl_6 species (**2a**, **7-*S*0**, and **7-*S*2**),[27] and even longer Ti_nCl_{3n}

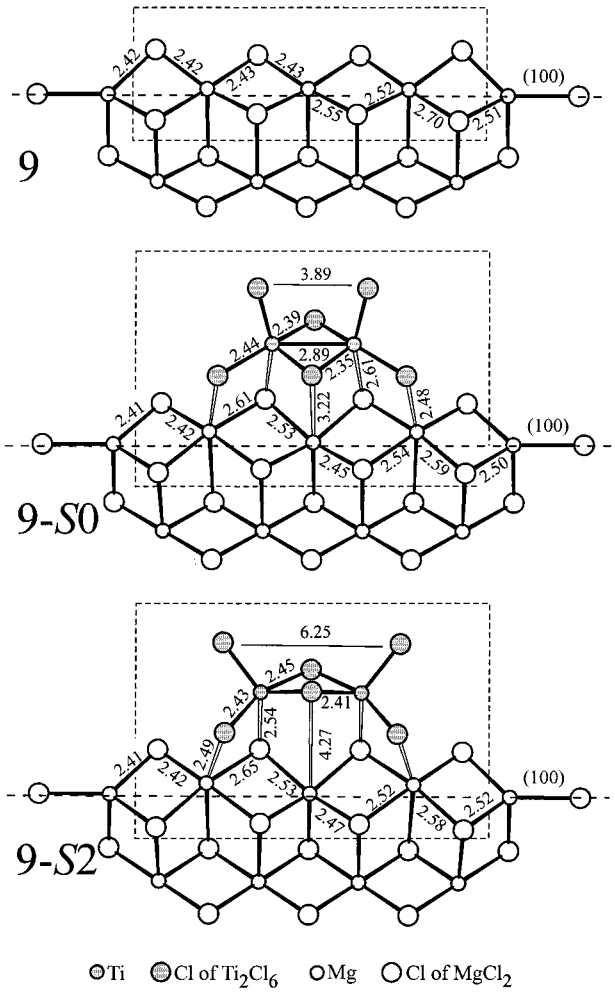

Figure 10. Optimized geometries of structures **9**, **9-*S*0**, and **9-*S*2**, corresponding to a Mg_9Cl_{18} cluster and to the Ti_2Cl_6 fragment adsorbed on the (100) face of a Mg_9Cl_{18} cluster, respectively. All the atoms enclosed in the dashed boxes have been optimized. Hollow bonds are used to indicate bonds between the Ti_2Cl_6 fragment and the Mg_9Cl_{18} cluster.

(e.g., **8-*S*0** or **8-*S*2**) species[17,18] are feasible. In fact, dimeric and tetrameric Ti(III) species are characterized by considerable bonding between the individual $TiCl_3$ fragments (positive E_{Intra}) which more than counterbalance, for this $MgCl_2$ lateral cut, the reduction of attractive interaction with the surface per Ti atom, with respect to the monomeric $TiCl_3$ species (negative ΔE_{Inter} in Table 1).

As discussed in ref 27, the relative amounts of monomeric and dimeric Ti species on the (100) cut of $MgCl_2$ are not only determined by their relative binding energy values. In fact, each dimeric species (Ti_2Cl_8 or Ti_2Cl_6) occupies only three coordination sites, corresponding to three Mg atoms, whereas two monomeric species ($2TiCl_4$ or $2TiCl_3$) occupy four sites, corresponding to four Mg atoms. Therefore, dimers are favored at high coverage of the surface (which can be achieved by adsorption of Ti species and possibly Lewis bases). This is also true for polynuclear Ti_nCl_{3n} species, which can be formed if atomic rearrangements of Ti(III) species could occur.

The prevalence of dimeric and polymeric Ti(III) species would be in line with the ESR silency of a large fraction of Ti(III).[13,17,18,20]

Stereoselectivity Implications. The Ti(III) monomers and the terminal titanium atoms of the Ti_mCl_{3m}

Scheme 1

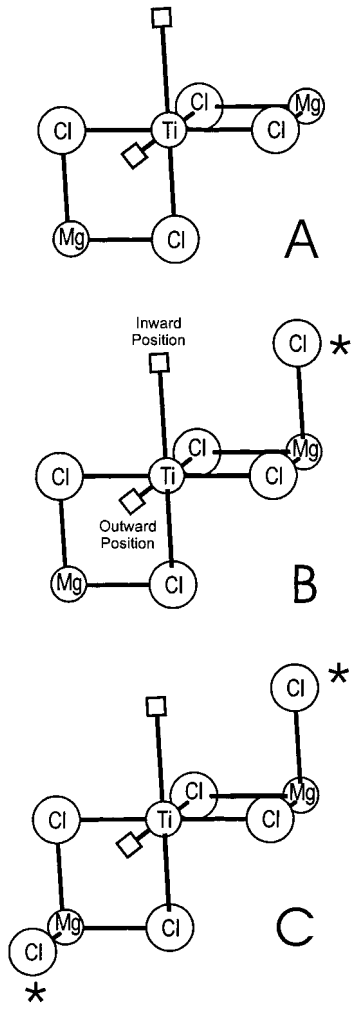

clusters are potential polymerization sites after alkylation of the dangling Ti−Cl bond. Instead, stable Ti(IV) species (excluding the monomer adsorbed on the (100) face) require the abstraction of a chloride anion in order to make place to the incoming monomer.

For a given active site, the local symmetry that characterizes the two coordination positions available to the growing chain and to the monomer is extremely relevant to determine the stereospecificity of the insertion reaction. Although alkylation and monomer coordination could lead to geometry changes, some insights into the possible stereoselectivity of the polymerization sites obtained by activation of the various Ti species can be safely obtained by inspection of the models.

First of all, we recall that molecular mechanics studies have shown that the stereoselectivity of these catalysts is not due to direct interactions of the chiral catalyst with the monomer, but to interactions between the chiral catalyst (one or two Cl atoms in this case) with the growing chain. These interactions force the chain to assume a chiral orientation, which, in turn, leads to a discrimination between the two prochiral faces of the propene monomer.[68,69] In Scheme 1 three different situations (A, B, C) are shown, which differ in the number (0 for A, 1 for B, 2 for C) of conditioning Cl atoms (marked by stars). Ti adsorbed species with structures substantially similar to structure A of Scheme 1 will be substantially aspecific, while those similar to structure B of Scheme 1 will be substantially nonstereoselective when the growing chain is outward coordinated, whereas will be substantially stereoselective when the growing chain is inward coordinated. Finally, Ti species similar to structure C of Scheme 1 should be substantially stereospecific, since both coordination positions available to the growing chain will be substantially stereoselective. It is worth noting that structures B and C of Scheme 1 correspond to the Cossee's C_1 model[70,71] and to the Allegra's C_2 model,[72] first developed for $TiCl_3$-based catalysts.

In this framework, a highly isotactic polymer cannot be produced by isolated monomeric species as, for instance, **1a**, **1b**, **1c**, **3a**, and **3b** as shown by molecular mechanics studies, since they lack conditioning chlorines, as structure A of Scheme 1.

Structures **5**, ***7-S2***, and **4**, instead, are more similar to the Cosse's C_1 model and resemble structure B of Scheme 1. The stereospecific behavior of structure ***7-S2*** has been investigated through molecular mechanics studies in the framework of the regular chain migratory mechanism for olefins polymerization.[68] These and analogous calculations on the C_1 symmetric homogeneous catalytic systems based on group 4 metallocenes[73,74] indicated that a regular back-skip of the growing chain to the coordination position previously occupied by the monomer at each step is required to ensure stereospecificity. In fact, by exchanging the relative positions of the growing chain and of the monomer, we switch from a highly stereoselective site (when the growing chain is coordinated close to the $MgCl_2$ surface, inward position) to a substantially nonstereoselective site (when the growing chain is coordinated far from the $MgCl_2$ surface, outward position). The driving force for a possible back-skip of the chain could be an energetic preference of the growing chain to occupy one of the two available coordination positions.[73,74] In this respect, it is worth noting that the presence of C_1 symmetric sites analogous to the homogeneous ones has been reported for heterogeneous Ziegler−Natta catalysts also.[24,26]

Among the models discussed in this paper, it can be seen that the terminal Ti of the linear clusters Ti_nCl_{3n} and the monomer adsorbed on the (110) face with both vicinal position saturated are very similar to Allegra's C_2 model, strongly reminds the classical C_2 symmetric homogeneous system based on metallocenes of group 4,[75] and substantially resembles structure C of Scheme 1. The enantioselective behavior of these systems was rationalized in the framework of the growing chain orientation mechanism.[69] The dimeric structure ***7-S0*** has a C_2-like local symmetry around the Ti atoms. This structure has not been investigated through nonbonded interactions, but it is reasonable to think that exchanging the relative positions of the growing chain and of the monomer, we switch from a highly stereoselective site (when the growing chain is inward coordinated) to a poorly stereoselective site (when the growing chain is outward coordinated). In fact, the dangling Cl atom in the almost axial position could induce a chiral orientation of the growing chain, but oscillations of this Cl atom in the relatively open environment could reduce the effectiveness of the steric control.

Finally, we want to remark that the stereoselective behavior can be easily modified by the presence of other species (internal and external donors in particular), which can either directly change the steric environment of the active species or modify the surface distri-

bution of adsorbed species with different stereospecificity. The latter mechanism favors both dimers[27] and linear clusters on the (100) face and lowers the number of monomers with vacant vicinal positions on the (110) face. Moreover, donors could saturate one or both of the vacant positions of a $TiCl_3$ fragment adsorbed on the (110) face and thus can influence directly the stereospecificity.

4. Conclusions

In this paper we attempted a systematic DFT investigation of the interactions possibly occurring between $TiCl_4$ molecules and $TiCl_3$ fragments with both (100) and (110) lateral cuts of $MgCl_2$ clusters. Models with a fixed geometry of the $MgCl_2$ support have been considered. However, we think that the energy differences found for different structures would be substantially confirmed by calculations with a more relaxed support. In effect, in the case of the Ti_2Cl_6 dimer, calculations on structures **9**, **9-*S*0**, and **9-*S*2**, in which a partial relaxation of the support was allowed, substantially confirmed the results obtained with the more rigid **7-*S*0** and **7-*S*2** structures. Thus, the following conclusions can be drawn:

(i) $TiCl_4$ molecules and $TiCl_3$ fragments are preferentially adsorbed on the (110) rather than on the (100) lateral cut of $MgCl_2$.

(ii) With respect to monomeric species, dimeric Ti_2Cl_8 on the (100) lateral cut is energetically favored, while Ti_2Cl_6 species are unfavored. These species are very similar to the models proposed by Cossee,[70,71] suggested by EXAFS studies,[8] and calculated to be possible isospecific site by molecular mechanics calculations.[27]

(iii) Besides monomeric and dimeric species, polynuclear Ti(III) species on the (100) lateral cut of $MgCl_2$ are possible and appear to be energetically favored, independent of the number of unpaired spins. This result supports the formation of polynuclear Ti chloride species first hypothesized by Brant and Speca[17,18] and could contribute to explain the ESR silency of a large fraction of Ti(III).[13,17,18,20]

The characterization of the various adsorbed Ti species is extremely relevant in terms of their potential stereospecific behavior in propene polymerization. It has to be noted that the several structures of similar energy we have found are consistent with a family of polymerization sites with different local symmetries (from C_1 to C_2-like to almost C_2), steric environment, and hence different stereospecific properties (from substantially aspecific sites to isospecific ones).

As far as the (100) face is concerned, dimeric Ti_2Cl_6 sites on the (100) cut are very similar to the C_1 symmetric sites proposed by Cossee,[70,71] while polynuclear Ti_nCl_{3n} sites with $n > 2$ are extremely similar to the C_2 symmetric sites proposed several years ago by Allegra for $TiCl_3$-based catalytic systems,[72] and present a strict analogy with the well-established models for isospecific polymerization with catalytic systems based on C_2 symmetric metallocenes.

On the (110) face there are many possibilities. In fact, although an isolated $TiCl_3$ molecule adsorbed on the (110) face can be thought to produce a poorly stereoregular polymer with a prevalence of syndiotactic diads,[76] C_1 and C_2 symmetric species, which can produce isotactoid and isotactic polymers, are obtainable by occupation of one and two vicinal positions. An easy switch between these three polymerization modes has been recently proposed on the basis of a high-resolution ^{13}C NMR microstructural analysis.[26]

This study is far from being comprehensive. In fact, the Ti species we have calculated can only represent a basis for the description of the real effective catalyst, since the relative distribution, interconversion, and stereospecificity of the various Ti species are sensitively modified by the presence of alkylaluminum compounds and, particularly, by the added Lewis bases. A study relative to the interaction between Lewis bases (1,3-diethers in particular) and the $MgCl_2$ support is reported elsewhere,[43] and further work is in progress.

In any case, we believe that the present study can represent a considerable improvement of our understanding of the interaction between the various Ti species and the $MgCl_2$ support, the two fundamental components of supported heterogeneous Ziegler−Natta catalysts.

Acknowledgment. We thank Prof. V. Busico of the University of Naples and scientists of Montell Polyolefins for useful discussions. This work has been supported by the Ministero della Ricerca Scientifica e Tecnologica of Italy within PRIN 1998 and 2000 fundings, and by Montell Polyolefins.

References and Notes

(1) Moore, E. P. J. *Polypropylene Handbook: Polymerization, Characterization, Properties, Applications*; Hanser Publishers: Munich, 1996.
(2) Natta, G. *Nobel Lectures in Chemistry, 1963−1970*; Elsevier: Amsterdam, 1972; p 27.
(3) Ziegler, K. *Nobel Lectures in Chemistry, 1963−1970*; Elsevier: Amsterdam, 1972; p 6.
(4) Kissin, Y. V. *Isospecific Polymerization of Olefins*; Springer-Verlag: New York, 1985.
(5) Giannini, U.; Giunchi, G.; Albizzati, E.; Barbè, P. C. Frontiers in Polymerization Catalysis 1987, NATO Advanced Research Workshop, Feb 1−6.
(6) Auriemma, F.; Talarico, G.; Corradini, P. In *Progress and Development of Catalytic Olefin Polymerization*; Sano, T., Uozumi, T., Nakatani, H., Terano, M., Eds.; Technology and Education Publisher: Tokyo, Japan, 2000; p 7.
(7) Jones, P. J. V.; Oldman, R. J. In *Etero EXAFS MgCl2*; Kaminsky, W., Sinn, H., Eds.; Springer-Verlag: Berlin, 1988; p 337.
(8) Popatov, A. G.; Kriventsov, V. V.; Kochubey, D. I.; Bukatov, G. D.; Zakharov, V. A. *Macromol. Chem. Phys.* **1997**, *198*, 3477.
(9) Magni, E.; Somorjai, G. A. *J. Phys. Chem. B* **1998**, *102*, 8788.
(10) Hasebe, K.; Mori, H.; Terano, M. *J. Mol. Catal.* **1997**, *124*, L1.
(11) Mori, H.; Hasebe, K.; Terano, M. *Macromol. Chem. Phys.* **1998**, *199*, 2709.
(12) Mori, H.; Sawada, M.; Higuchi, T.; Hasebe, K.; Otsuka, N.; Terano, M. *Macromol. Rapid Commun.* **1999**, *20*, 245.
(13) Chien, J. C. W.; Wu, J. C. *J. Polym. Sci., Part A: Polym. Chem.* **1982**, *20*, 2461.
(14) Chien, J. C. W.; Hu, Y. *J. Polym. Sci., Part A: Polym. Chem.* **1989**, *27*, 897.
(15) Sergeev, S. A.; Polubayarov, V. A.; Zakharov, V. A.; Anufrienko, U. F.; Bukatov, G. D. *Makromol. Chem.* **1985**, *186*, 243.
(16) Weber, S.; Chien, J. C. W.; Hu, Y. *J. Polym. Sci., Part A: Polym. Chem.* **1989**, *27*, 1499.
(17) Brant, P.; Speca, A. N. *Macromolecules* **1987**, *20*, 2740.
(18) Brant, P.; Speca, A. N.; Johnston, D. C. *J. Catal.* **1988**, *113*, 250.
(19) Kashiwa, N.; Yoshitake, J. *Makromol. Chem.* **1984**, *185*, 1133.
(20) Fuhrmann, H.; Herrmann, W. *Macromol. Chem. Phys.* **1994**, *195*, 3509.
(21) Busico, V.; Corradini, P.; De Martino, L. *Makromol. Chem., Rapid Commun.* **1990**, *11*, 49.
(22) Paukkeri, R. V. T.; Lehtinen, A. *Polymer* **1993**, *34*, 2488.
(23) Busico, V.; Cipullo, R.; Corradini, P.; Landriani, L.; Vacatello, M.; Segre, A. L. *Macromolecules* **1995**, *28*, 1887.

(24) Busico, V.; Cipullo, R.; Talarico, G.; Segre, A. L.; Chadwick, J. C. *Macromolecules* **1997**, *30*, 4787.
(25) Randall, J. C. *Macromolecules* **1997**, *30*, 803.
(26) Busico, V.; Cipullo, R.; Monaco, G.; Talarico, G.; Vacatello, M.; Chadwick, J. C.; Segre, A. L.; Sudmeijer, O. *Macromolecules* **1999**, *32*, 4173.
(27) Corradini, P.; Barone, V.; Fusco, R.; Guerra, G. *Gazz. Chim. Ital.* **1983**, *113*, 601.
(28) Corradini, P.; Busico, V.; Guerra, G. *Comprehensive Polymer Science*; Allen, G., Bevington, J. C., Eds.; Pergamon Press: Oxford, 1989; Vol. 4, pp 29−50.
(29) Zambelli, A. L. P.; Bajo, G.; Bovey, F. A. *Macromolecules* **1975**, *8*, 687.
(30) Cavallo, L.; Guerra, G.; Corradini, P. *J. Am. Chem. Soc.* **1998**, *120*, 2428.
(31) Fujimoto, H.; Yamasaki, T.; Mizutani, H.; Koga, N. *J. Am. Chem. Soc.* **1985**, *107*, 6157.
(32) Jensen, V. R.; Børve, K. J.; Ystenes, M. *J. Am. Chem. Soc.* **1995**, *117*, 4109.
(33) Sakai, S. *J. Phys. Chem.* **1994**, *98*, 12053.
(34) Sakai, S. *Int. J. Quantum Chem.* **1997**, *65*, 739.
(35) Puhakka, E.; Pakkanen, T. T.; Pakkanen, T. A. *Surf. Sci.* **1995**, *334*, 289.
(36) Puhakka, E.; Pakkanen, T. T.; Pakkanen, T. A.; Iiskola, E. *J. Organomet. Chem.* **1996**, *511*, 19.
(37) Puhakka, E.; Pakkanen, T. T.; Pakkanen, T. A. *J. Mol. Catal.* **1996**, *120*, 143.
(38) Puhakka, E.; Pakkanen, T. T.; Pakkanen, T. A. *J. Chem. Phys.* **1997**, *101*, 6063.
(39) Puhakka, E.; Pakkanen, T. T.; Pakkanen, T. A. *J. Mol. Catal.* **1997**, *123*, 171.
(40) Boero, M.; Parrinello, M.; Terakura, K. *J. Am. Chem. Soc.* **1998**, *120*, 2746.
(41) $TiCl_3$ does not exist as an isolated molecule in the conditions used in Ziegler−Natta catalysis. However, Ti(III) species adsorbed on the $MgCl_2$ support are clearly feasible after reduction of adsorbed $TiCl_4$ molecules.
(42) Barbé, C.; Cecchin, G.; Noristi, L. *Adv. Polym. Sci.* **1987**, *81*, 1.
(43) Toto, M.; Morini, G.; Guerra, G.; Corradini, P.; Cavallo, L. *Macromolecules* **2000**, *33*, 1134.
(44) Partin, D. E.; O'Keeffe, M. *J. Solid State Chem.* **1991**, *95*, 176.
(45) ADF 2.3.0, User Guide Vrije Universiteit Amsterdam, Amsterdam, The Netherlands, 1996.
(46) Baerends, E. J.; Ellis, D. E.; Ros, P. *Chem. Phys.* **1973**, *2*, 41.
(47) te Velde, B.; Baerends, E. J. *J. Comput. Phys.* **1992**, *99*, 84.
(48) Versluis, L.; Ziegler, T. *J. Chem. Phys.* **1998**, *88*, 322.
(49) Snijders, J. G.; Vernooijs, P.; Baerends, E. J. *At. Nucl. Data Tables* **1981**, *26*, 483.
(50) Vosko, S. H.; Wilk, L.; Nusair, M. *Can. J. Phys.* **1980**, *58*, 1200.
(51) Becke, A. *Phys. Rev. A* **1988**, *38*, 3098.
(52) Perdew, J. P. *Phys. Rev. B* **1986**, *33*, 8822.
(53) Perdew, J. P. *Phys. Rev. B* **1986**, *34*, 7406.
(54) Margl, P. M.; Ziegler, T. *Organometallics* **1996**, *15*, 5519.
(55) Margl, P. M.; Ziegler, T. *J. Am. Chem. Soc.* **1996**, *118*, 7337.
(56) Willis, B. G.; Jensen, K. F. *J. Phys. Chem. A* **1998**, *102*, 2613.
(57) Jensen, V. R.; Børve, K. J. *J. Comput. Chem.* **1998**, *19*, 947.
(58) Nayak, S. K.; Jena, P. *J. Am. Chem. Soc.* **1999**, *121*, 644.
(59) Jacobsen, H.; Ziegler, T. *J. Am. Chem. Soc.* **1994**, *116*, 3667.
(60) Ritter, E.; Kvisle, S.; Nirisen, Ø.; Ystenes, M.; Øye, H. A. In *Transition Metal Catalyzed Polymerization: Ziegler−Natta and Metathesis Polymerization*; Quirk, R. P., Ed.; Cambridge University Press: Cambridge, 1988; p 292.
(61) Lee, C.; Yang, W.; Parr, R. G. *Phys. Rev. B* **1988**, *37*, 785.
(62) To further investigate these somewhat different conclusions, we optimized a 5-fold coordinated structure by fixing the Ti−Cl(surface) distance to 3.20 Å (which is the Ti−Cl(surface) distance found for a $TiCl_4$ molecule adsorbed on the (100) $MgCl_2$ face). The optimized 5-fold geometry is higher in energy by only 2.1 kcal/mol relative to **3b**, indicating a substantially flat potential energy surface. It is reasonable that different levels of theory can give quite different results in such cases.
(63) Novaro, O.; Blaisten-Barojas, E.; Clementi, E.; Giunchi, E.; Ruiz-Vizcaya, M. E. *J. Chem. Phys.* **1978**, *68*, 2337.
(64) The very short Ti−Ti bond distance we calculated for **6-*S*0** is in a good agreement with the Ti−Ti distances found by Cotton and Wojtczak[65] in the diamagnetic complexes $Ti_2Cl_2[H_5C_6NC(H)NC_6H_5]_4$ and $Ti_2Cl_2[H_9C_{12}NC(H)NC_{12}H_9]_4$ (Ti−Ti = 2.899 and 2.916 Å, respectively). Differently, the Ti−Ti distance we calculated for **6-*S*2** is too short when compared to the Ti−Ti distances found in the paramagnetic complexes Ti_2Cl_6[1,2-bis(diisopropylphospino)ethane]$_2$[66] and $Ti_2Cl_6[P(CH_3)_3]_4$[65] (Ti−Ti = 3.438 and 3.704 Å). To check the performances of the methodology we used, we optimized the structure of the $Ti_2Cl_6(PH_3)_4$ complex with two unpaired electron spins, and we calculated the Ti−Ti distance to be equal to 3.77 Å, in very good agreement with the experimental value for $Ti_2Cl_6[P(CH_3)_3]_4$. It is worthy to note that a geometry optimization of the $Ti_2Cl_6(PH_3)_4$ complex without gradient corrections gives a Ti−Ti distance equal to 3.18 Å.
(65) Cotton, F. A.; Wojtczak, W. A. *Gazz. Chim. Ital.* **1993**, *123*, 499.
(66) Hermes, A. R.; Girolami, G. S. *Inorg. Chem.* **1990**, *29*, 313.
(67) Clearly, Ti_4Cl_{12} species with two unpaired electron spins could have been considered as well. However, they are not needed for the present general discussion.
(68) Corradini, P.; Barone, V.; Fusco, R.; Guerra, G. *Eur. Polym. J.* **1979**, *15*, 1133.
(69) Corradini, P.; Barone, V.; Fusco, R.; Guerra, G. *J. Catal.* **1982**, *77*, 32.
(70) Arlman, E. J.; Cossee, P. *J. Catal.* **1964**, *3*, 99.
(71) Cossee, P. *J. Catal.* **1964**, *3*, 80.
(72) Allegra, G. *Makromol. Chem.* **1971**, *145*, 235.
(73) Guerra, G.; Cavallo, L.; Moscardi, G.; Vacatello, M.; Corradini, P. *Macromolecules* **1996**, *26*, 4834.
(74) Rieger, B.; Jany, G.; Fawzi, R.; Steimann, M. *Organometallics* **1994**, *13*, 647.
(75) Brintzinger, H. H.; Fischer, D.; Mülhaupt, R.; Rieger, B.; Waymouth, R. M. *Angew. Chem., Int. Ed. Engl.* **1995**, *34*, 1143.
(76) Corradini, P.; Guerra, G.; Barone, V. *Eur. Polym. J.* **1984**, *20*, 1177; see particularly Figures 6 and 9.

MA000988H